

Solid Phase Extraction and Determination of Cationic Azo Dye from Aqueous Solution Using Dried Papyrus Plant

A. M. El-Wakil¹, W. M. Abou El-Maaty², F. S. Awad³, A. A. Oudah⁴

^{1,2,3,4} Chemistry Department, Faculty of Science, P.O.Box: 35516, Mansoura University, Mansoura, Egypt

Abstract: The dried papyrus plant (DP) treated with 0.025 M ethylenediaminetetraacetic acid (EDTA) at pH=10 was used as effective adsorbent for the removal of Methylene Blue (MB) (cationic azo dye) from aqueous solution. The dried papyrus plant sample characterized by Fourier Transform Infrared (FTIR), and Scanning Electron Microscopy (SEM). The effects of initial dye concentration (5-250 mg/L), pH (2-10), temperature (298-318 K), adsorbent dose (0.005-0.035 g), and contact time were investigated and discussed. The batch adsorption experiments, showed that the maximum adsorption of MB ($q_{e_{max}}$) at pH=8 was 101.60 mg/g and increased with the increase in temperature from 298 to 318 K. The adsorption of MB onto (DP) reached equilibrium within about 150 min. The adsorption equilibrium is described using Langmuir and Freundlich isotherm models. It can be found that the regression coefficient R^2 obtained from Langmuir model is much higher than that from Freundlich model and the practical adsorption capacity is very close to that calculated from Langmuir isotherm, suggesting that the Langmuir isotherm fits better with the experimental data. The adsorption kinetics followed a pseudo-second order kinetic model and intra particle diffusion was involved in the adsorption process. Thermodynamic results indicated that the adsorption process was spontaneous and endothermic in nature. The proposed adsorbent was successfully applied for the removal of MB from aqueous solution with a percent recovery 81.65 % by using 0.1 N HCl.

Keywords: Papyrus Plant, Methylene Blue, Adsorption, Desorption, SEM.

1. Introduction

With the revolution in textile and similar industries in Egypt, the colored effluents due to the use of organic dyes such as Methylene Blue for dyeing silk, cotton, leather, wool, paper and other final products [1, 2]. This is one of major problems concerning textile waste waters. This colored effluents has large amounts of suspended organic solids which are harmful to human being and toxic for organism [3].

The removal of these dyes from waste water has a considerable attention over the past decades to decrease their impact on the environment. Amongst the numerous techniques of dye removal, adsorption is a well-known equilibrium separation process and an effective method for water decontamination applications.

Physical adsorption technology, i.e., by activated carbons [4] has been found to be an efficient technology for decolorization of wastewater. Although the removal of dyes through adsorption is quite effective, its use is sometimes restricted due to the high cost of activated carbon and the difficulties associated with regeneration.

In recent years, attention has been shifted towards the materials which are byproducts or wastes from large scale industrial operations and agricultural waste materials. A wide variety of low cost materials, have been exploited for the removal of dyes from aqueous solutions, including lemon peel [5], sugarcane dust [6], jute fiber [7], oil palm [8], orange peel [9], coir pith [10], cotton seed shell [11], beech sawdust [12], ground nut shell [13], corn stalks and corn cobs [14]. The major advantages of these materials include: low cost, high efficiency, minimization of chemical or biological sludge, no additional nutrient requirement, and regeneration of sorbent and possibility of effluent recovery.

Cyperus papyrus [15, 16] originated in Central Africa and has spread over tropical Africa. It has been cultivated in Egypt and neighboring areas since ancient times and is sometimes naturalized in the Mediterranean area. Nowadays it is widely grown as an ornamental. Papyrus fiber contains 54–68% cellulose and 24–32% lignin.

The main focus of this study was to evaluate the capacity of dried papyrus plant (DP) adsorbent for the removal of methylene blue as a model compound for basic dyes. The effects of pH, contact time, initial dye concentration and adsorbent dosage on the adsorption capacity were investigated. Moreover, kinetic and equilibrium models were used to fit experimental data.

2. Experimental

Materials and Reagents

Methylene blue (MB)

MB is a synthetic cationic thiazine dye of an amorphous nature with a molecular formula $C_{16}H_{18}ClN_3S \cdot xH_2O$. It is also called basic blue 9 and tetramethylthionine chloride with colour index (CI) number 52015. The molecular weight of MB is 320 and its maximum wave length 662 nm. It is a dark green powder, with a characteristic deep blue colour in aqueous solution where it dissociates into an MB cation and a chloride anion. Methylene blue (MB) was supplied by Sigma-Aldrich. MB stock solution 1000 ppm was prepared by dissolving accurately 1g of MB in distilled water up to the mark of 1L of measuring flask. Methylene blue solutions of lower concentrations were prepared by further dilution with distilled water.

Acetate buffer (pH = 4 – 6)

Buffer solution of CH₃COOH/CH₃COONa was prepared by titration of 0.1 M of CH₃COOH against 0.1 M NaOH until the required pH is reached. The pH value was monitored using pH meter.

Phosphate buffer (pH = 2-3, 7-12)

Buffer solution of H₃PO₄/ NaH₂PO₄ was prepared by titration of 0.1 N of NaH₂PO₄ against 0.1 M HCl (for pH range 2 – 3) or against 0.1 N NaOH (for pH range 7 – 12) until the required pH is reached. The pH value was monitored using pH meter.

Preparation of dried papyrus plant (DP):

The papyrus plant was collected from Manzala Lake in Mansoura, Egypt. The roots of the plant were removed while the leaves and stems were washed several times with tap water then with distilled water and were immersed in 0.025 M EDTA at pH 10 for 24 hour for removing any metal ions adsorbed on the plant and washed with distilled water for several times and dried in oven at 110 °C for 48 h then ground and stored in desiccators till used in adsorption experiments.

Batch equilibrium and kinetic studies

Batch sorption experiments were done by shaking 0.025 g of DP adsorbent with 25 ml aqueous solution of Methylene Blue (MB) in 100 ml-Erlenmeyer flasks placed in a temperature controlled shaking water bath at different concentrations (between 5 and 250 mg/l), pHs (between 2 and 10), temperature (298-323 K), adsorbent dose (0.005-0.035 g), at a constant shaking rate of about 200 rpm. The amounts of dye removed by sorbents q_e and percent extracted % E can be calculated using the following equations:

$$\text{Extraction \%} = \frac{(C_0 - C_e)}{C_0} \times 100 \quad (1)$$

$$q_e = \frac{(C_0 - C_e) V}{m} \quad (2)$$

Where q_e is the amount of dye adsorbed (mg/g). C₀ and C_e are the initial and equilibrium liquid-phase concentrations of dye (mg/g), respectively. V is the volume of the solution (L), and m is the weight of the sorbent used (g).

Adsorption Kinetic Studies

The adsorption kinetics of MB onto DP adsorbent were measured at initial concentration of 200 ppm. 200 ml of aqueous methylene blue solutions was introduced into a 500 ml conical flask and mixed with 0.2 g of the adsorbent. The solution was stirred continuously at 25 °C and 1 ml of solution were taken at different time intervals (0 – 1440) min. The concentration of MB was analyzed spectrophotometrically using UV-Vis spectrophotometer at wavelength 554 nm and the amount of adsorption q_t was calculated according to equation (2).

Desorption Studies

For the desorption studies, 0.025g adsorbent was loaded with MB 25 ml of 200 ppm dye solution at pH = 8. Then, the dye-loaded adsorbent was collected and treated with 25 ml of x M HCl to remove the adsorbed dye. The desorption efficiency was calculated using the following equation:

Desorption % = Amount released to solution (ppm) / Total Adsorbed (ppm)

3. Result and Discussion

Characterization of prepared adsorbent Scanning electron microscopy (SEM):

Micrograph of DP was obtained using scanning electron microscope. The SEM micrograph obtained clearly indicate the porous structure of dried papyrus plant (DP) adsorbent at magnification of 300x as shown in Fig 1.

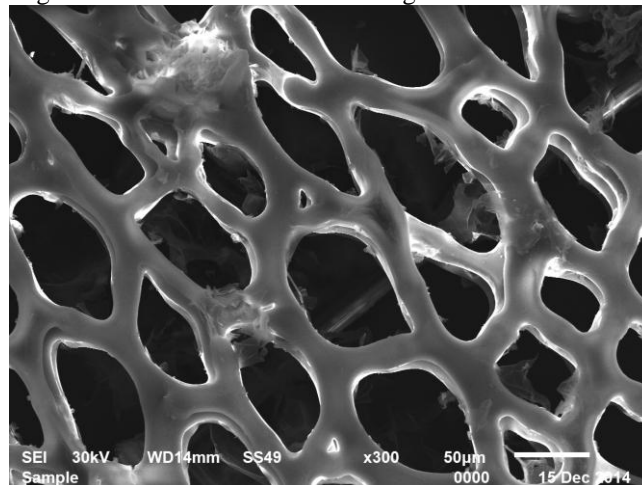


Figure 1: shows FTIR spectra for dried papyrus sample

FTIR spectroscopy

FTIR spectra were recorded between 4000 and 100 cm⁻¹ using a Mattson 5000 FTIR spectrometer. Discs were prepared by first mixing 1 mg dried papyrus with 500 mg of KBr (Merck for spectroscopy) in an agate mortar and then pressing the resulting mixture at 5 ton / cm² for 5 min and 10 ton /cm² for 5 min under vacuum. Observation of the absorption bands [17, 18] as shown in Fig 2. and table 1 show the appearance of a sharp absorption peak at 1744 Cm⁻¹ indicates the abundant introduction of carboxyl group due to modification using EDTA.

Function group	Wave Number (Cm ⁻¹)
O-H stretching mode of hexagonal group	3442 Cm ⁻¹
Aliphatic (C-H)	2848-2917 Cm ⁻¹
C=C stretching in aromatic ring	Near 1600 Cm ⁻¹
C-O bonds such as those in ethers, phenols, and esters	1300-1000 Cm ⁻¹
Highly conjugated (C=O stretching, C-O stretching in carboxylic groups and carboxylic moieties.	Weak bands at 1259, and 1629 Cm ⁻¹
(C=O) stretching vibrations of carboxyl groups (due to physical adsorption of EDTA)	Band at (1741 Cm ⁻¹)

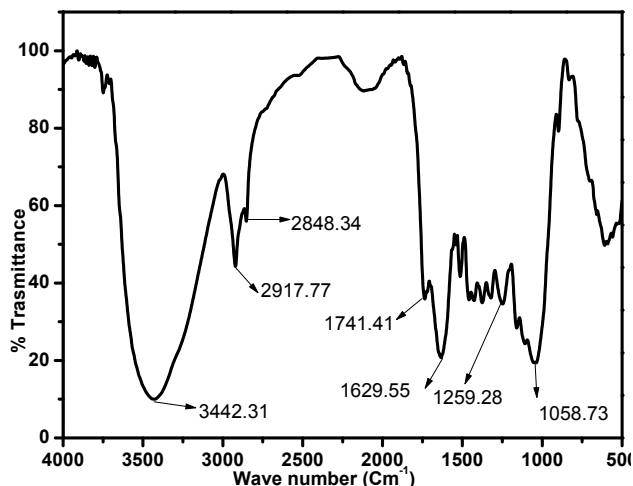


Figure 2: Shows FTIR spectra for dried papyrus sample.

Effect of pH on MB adsorption

Effect of pH on the removal of (MB) by DP is presented in Fig 3. It revealed that the percent of dye removal increased as the initial pH of the dye solution was increased from (2 to 10) and maximum adsorption of MB occur at pH 8. However, the uptake capacity does not change significantly from pH 8.0 to 10.0 and the removal efficiency (%E) is kept practically constant (variations lower than 2.0%). When the pH increases from pH=2 to pH=10, the percent of MB removal by DP from 0.33 % to 34.74 %. The adsorption of MB onto dried papyrus plant is affected by the characteristics of the adsorbent surface (comprised various functional groups such as carboxyl hydroxyl and carbonyl groups confirmed qualitatively using FTIR) and the structure of dye molecule. Therefore, at various pH values, electrostatic attraction as well as the ionic properties and structure of dye molecules and adsorbent surface could play very important roles in the dye adsorption on adsorbents. Lower adsorption of MB at acidic pH is probably due to the presence of excess H⁺ ions competing with the MB dye for the active sites.

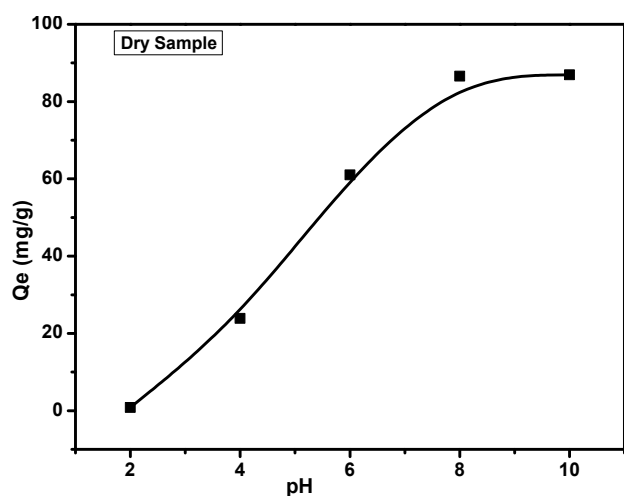


Figure 3: Effect of the pH values on adsorption capacity of MB by DP. (Conditions: C₀ = 250 mg/L, T=25°C; adsorbent dose = 0.025 g/25 ml).

Effect of initial concentration on adsorption of MB

The dye uptake onto DP as a function of initial MB concentration is shown in Fig 3. It is revealed that, by increasing the initial dye concentration in test solution the amount of MB adsorbed per unit mass of adsorbent increase. When the initial concentration of MB increases from 5 to 250 mg/l at 25 °C, The amount of MB adsorbed at equilibrium (q_e) increase from 4.88 to 101.60 mg/g for DS adsorbent. This may be attributed to the fact that the increase of the initial concentration of the adsorbate represents a driving force to overcome the mass transfer resistance of dye between the aqueous and solid phases.

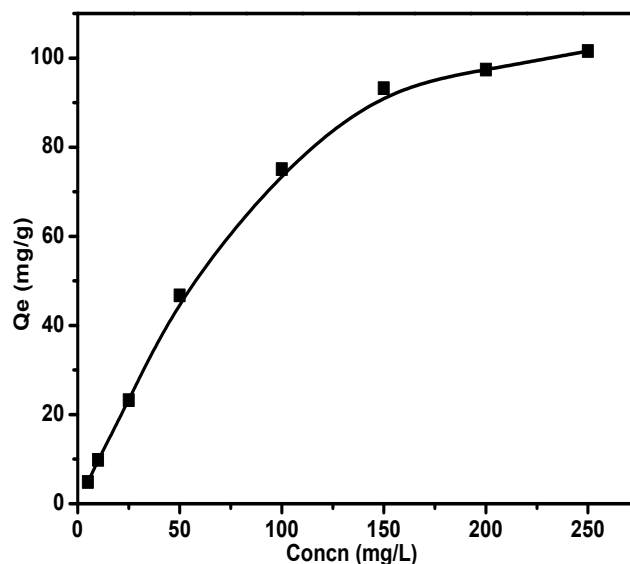


Figure 3: Effect of initial concentration on adsorption capacity of MB by DP. (Conditions: C = 5 - 250 mg/L, T=25°C; adsorbent dose = 0.025 g/25 ml).

Effect of contact time on MB adsorption

The effect of contact time on adsorption capacity of DP for MB is shown in Fig 4. It is clear that the adsorption capacity of DP adsorbent increased rapidly with the increase of contact time from 0 to 45 min and more than 60% of the equilibrium adsorption capacity for MB occurred within 10 min and then the adsorption rate decreased gradually and after 150 min, the adsorption capacity became constant and the adsorption reached equilibrium. Therefore, 150 min was selected as the contact time for the adsorption of MB onto the adsorbents under our experimental conditions. The fast adsorption at the initial stage may be due to the higher driving force making fast transfer of MB ions to the surface of adsorbent particles and the availability of the uncovered surface area and the remaining active sites on the adsorbent. At this stage, more than 60% of MB adsorption was found in all cases. The second stage was slower, possibly because many of the available external sites was already occupied and because of the slow diffusion of MB molecules into the pores of different adsorbents. After 2.5 h, the uptake was almost constant such that it could be considered the equilibrium time of the MB adsorption. To ensure that sufficient contact time was obtained, further adsorption experiments were carried out for 7h.

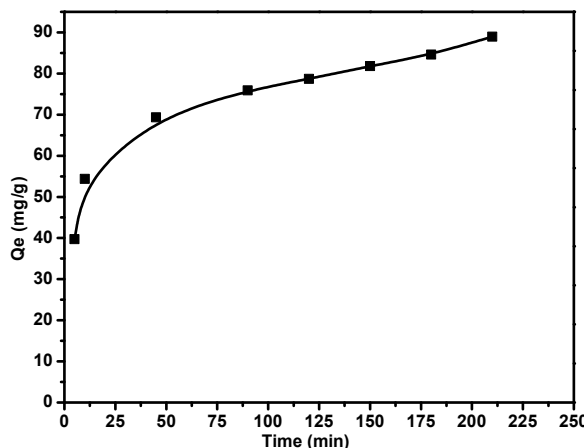


Figure 4: Effect of the contact time on adsorption capacity of DP adsorbents at initial concentration 200 ppm for MB. (Conditions: T=25 °C; adsorbent dose = 0.2 g/200 ml; pH= 8)

Effect of adsorbent dosage

The effect of amount of DP adsorbent on the removal percentage of MB was shown in Fig 5. It could be clearly seen that, an increase in sorbent dose is in favor of dye removal. When the sorbent dose increases from 0.005-0.035 g, the percent MB dye removals by DP from 20.79 to 78.01. It was observed that the percent removal of MB gradually increased with further increase in adsorbent up to 0.03 g and thereafter remained unchanged. The percent removal of MB increased is basically due to the number of active sites and available surface area increase with dosage. The optimum dose was found to be 1.0 g/L. However, the amount of MB adsorbed (mg/g) was found to decrease with further increase in adsorbent dosage. The decrease in adsorption density with increase in the adsorbent dose is mainly due to unsaturation of adsorption sites through the adsorption reaction, another reason may be due to the particle interactions such as aggregation resulting from high adsorbent concentration such aggregation would lead to a decrease in the total surface area of adsorbent.

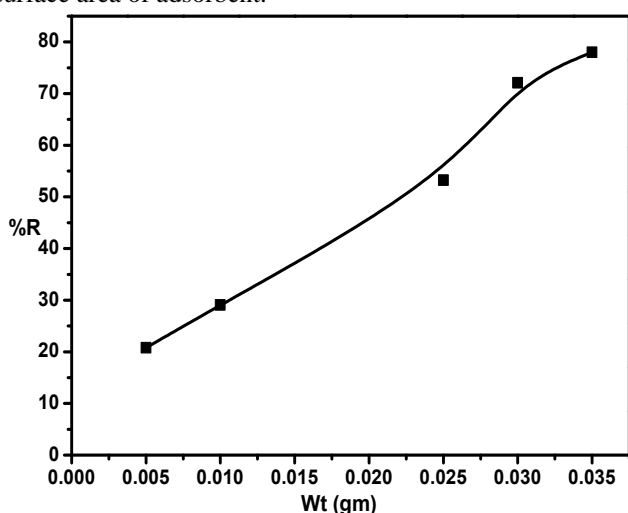


Figure 5: Effect of dose on adsorption capacity of DP adsorbents at initial concentration 200 ppm for MB. (Conditions: T=25 °C; adsorbent dose = 0.005 - 0.035 g; pH= 8)

Effect of temperature on adsorption of MB

The effect of temperature on the adsorption rate of MB on DP was investigated at three different temperatures (298, 308, and 318 K) using initial concentration of 100–250 mg/L (Fig. 6). The major effect of temperature is influence by the diffusion rate of adsorbate molecules and internal pores of the adsorbent particle. It is observed that the equilibrium adsorption uptake increases with increased temperature at all concentrations studied. An increase of temperature increases the rate of diffusion of the adsorbate molecules across the external boundary layer and within the internal pores of the adsorbent particle, due to decrease in the viscosity of the solution [19]. When the temperature increased from 298 to 318 K, the maximum adsorption capacities of MB removed by DP are found to be increased from 101.60 to 155.80. This phenomenon indicates that the adsorption process is endothermic in nature. This may be due to the mobility of molecules which increases generally with a rise in temperature [20].

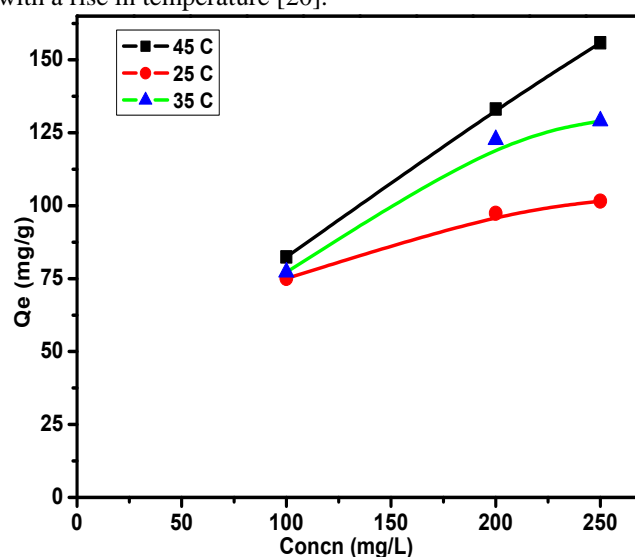


Figure 6: Effect of temperature on adsorption capacity of DP adsorbent for MB. (Conditions: C= 100-250 ppm; T=25 °C; adsorbent dose = 0.025/25 ml; pH= 8).

Adsorption isotherms

The adsorption isotherm is very useful to describe how the adsorption molecules distribute between the liquid phase and the solid phase when the adsorption process reaches an equilibrium state. The adsorption isotherm data were fitted by the two most used models, the Freundlich and Langmuir models. The parameters obtained from the two models provide important information on the sorption mechanism and the surface property and affinity of the adsorbent

The Langmuir isotherm assumes a surface with homogeneous binding sites equivalent sorption energies, and no interaction between adsorbed species. Its mathematical form is written as [21-22]:

$$\frac{C_e}{q_e} = \frac{1}{Q_b} + \frac{C_e}{Q} \quad (3)$$

Where q_e is the amount adsorbed at equilibrium (mg g^{-1}), C_e is the equilibrium concentration of the MB (mg L^{-1}), constant b is related to the energy of adsorption (Lmg^{-1}), Q is the Langmuir monolayer adsorption capacity (mg g^{-1}). The

essential characteristics of the Langmuir equation can be expressed in terms of a dimensionless separation factor R_L [23].

$$R_L = \frac{1}{1 + bC_0} \quad (4)$$

C_0 is the highest initial solute concentration, b is Langmuir adsorption constant (L/mg), R_L indicates the type of isotherm to be reversible ($R_L = 0$), Favorable ($0 < R_L < 1$), Linear ($R_L = 1$) or unfavorable ($R_L > 1$) [23].

The Freundlich isotherm is an empirical equation based on an exponential distribution of adsorption sites and energies. It is represented as [24, 25]

$$\ln q_e = \ln K_f + \frac{1}{n} \ln C_e \quad (5)$$

Where q_e is the amount adsorbed at equilibrium (mg g^{-1}), C_e is the equilibrium concentration of the MB (mg L^{-1}), K_f is

roughly an indicator of the adsorption capacity, and $1/n$ is the adsorption intensity. A linear plot of $\ln q_e$ versus $\ln C_e$ confirms the validity of the Freundlich model.

Fig. 7. and Fig. 8. Show the linear plot of Langmuir and Freundlich isotherm models for MB, respectively. The equilibrium parameters calculated from Langmuir and Freundlich isotherm equations are presented in (Table 2 and Table 3.) .It is noticed that the value of R_L is 0.02 indicating that the adsorption is a favorable process. It can be found that the regression coefficient R^2 obtained from Langmuir model is much higher than that from Freundlich model, suggesting that the Langmuir isotherm fits better with the experimental data. The practical adsorption capacity is very close to that calculated from Langmuir isotherm model suggesting that, the adsorption process are favorable for MB under conditions used in this study.

Table 2: Parameters of langmuir isotherm for adsorption of MB by DP.

Adsorbents	Langmuir parameters				
	R^2	b (L/mg)	$Q_{max, fitted}$	Q_{exp}	R_L
DP	0.99	0.21	103.30	101.60	0.02

Table 3: Parameters of Freundlich isotherm for adsorption of MB by DP.

Adsorbents	Freundlich parameters		
	R^2	K_f	$1/n$
DP	0.93	17.46	0.40

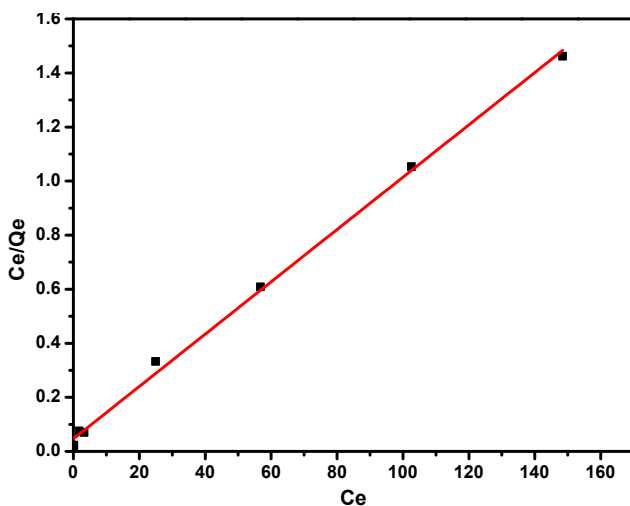


Figure 7: Langmuir plot for the adsorption of MB by DP

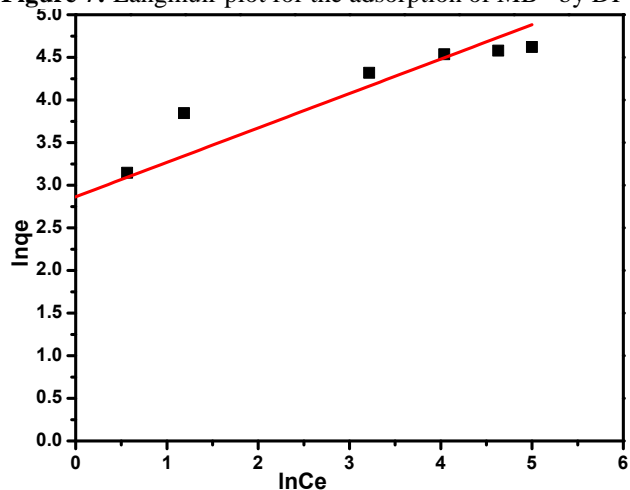


Figure 8: Freundlich plot for for the adsorption of MB by DP

Adsorption Kinetics

Pseudo-first and pseudo-second order kinetics models Adsorption kinetics is one of the most important parameters for the evaluation of adsorption efficiency. Two main kinetic models namely the pseudo-first order and pseudo-second order were used in this study to characterize adsorption kinetics [23, 24]. Non-linear fitting methods were applied using the Origin 7.0© software.

The pseudo-first order kinetics is given by the equation:

$$\log(q_e - q_t) = \log q_e - \frac{K_1 t}{2.303} \quad (6)$$

Where q_e and q_t are the amounts of mercury adsorbed (mg g^{-1}) at equilibrium and at time t (min), respectively, and k_1 the rate constant of adsorption (min^{-1}). Values of k_1 were calculated from the plots of $\ln(q_e - q_t)$ versus t (fig.9) at initial concentration of 200 ppm of MB.

The second-order kinetic model is expressed as:

$$\frac{t}{q_t} = \frac{1}{K_2 q_e^2} + \frac{t}{q_e} \quad (7)$$

Where k_2 is the rate constant of second-order adsorption ($\text{g mg}^{-1} \text{min}^{-1}$). Values of k_2 and q_e were calculated from the intercept and slope of the plots of t/q_t versus t . The linear plots of t/q_t versus t (Fig. 10) .The derived kinetic model parameters for MB adsorption onto DP are shown in Table 4. As can be seen by the values for R^2 and agreement between experimental and calculated q_e values, the pseudo-second order kinetic model fits the experimental results more accurately than the pseudo-first order kinetic model (Table 5). Thus, it can be concluded that MB adsorption on DP follows the pseudo-second order rate equation. This fact suggests that the rate of sorption for DP is dependent on the availability of the sorption sites rather than the concentration of the adsorbate in the bulk solution.

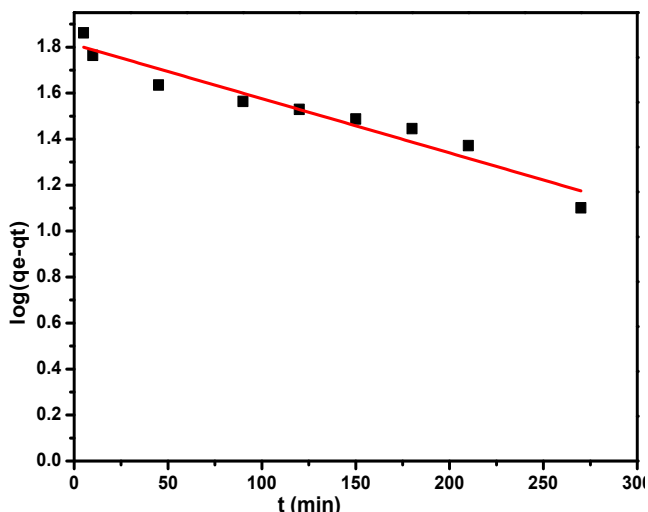


Figure 9: Pseudo- First-order kinetic model for adsorption of MB by DP.

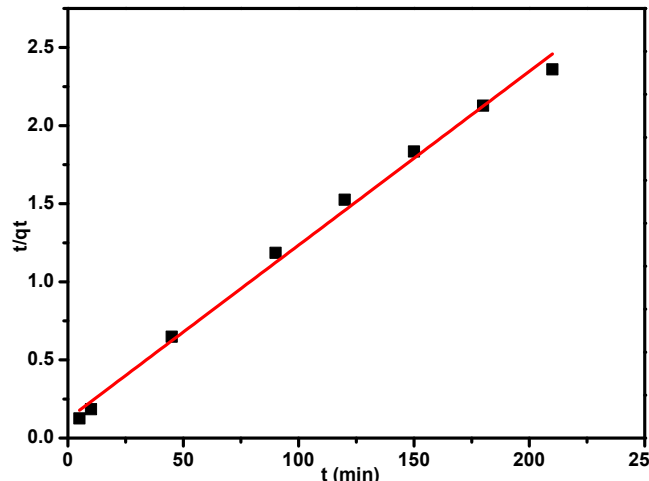


Figure 10: Pseudo-second-order kinetic model for adsorption of MB by DP.

Table 4: Parameters of first order kinetic model for adsorption of 200 ppm MB by DP

Adsorbent code	Pseudo-first order			
	$q_e \text{ exp. mg.g}^{-1}$	$q_e \text{ cal. mg.g}^{-1}$	$K_1 (\text{min}^{-1})$	R^2
DP	101.6	64.71	0.0054	0.93

Table 5: Parameters of second order kinetic model for adsorption of 200 ppm MB by DP

Adsorbent Code	$q_e \text{ exp. mg.g}^{-1}$	$q_e \text{ cal. mg.g}^{-1}$	$K_2 \text{ g.mg}^{-1} \text{ .min}^{-1}$	R^2
DP	101.60	100	8.19×10^{-4}	0.99

Intra particle diffusion model

Intra-particle diffusion mechanism was studied to investigate the diffusion mechanism of adsorption process by Weber and Morris equation. The linear form of intra-particle diffusion model was given by [24]:

$$q_t = k_D t^{0.5} + c \quad (8)$$

Where C was the intercept and k_D was the intra-particle diffusion rate constant ($\text{mg g}^{-1} \text{ min}^{-0.5}$).

If intra-particle diffusion was involved in the adsorption, then a plot of q_t against $t^{1/2}$ would result in a linear relationship that allows calculation of the value of k_D from the slope. The C intercept values give an idea of the boundary layer thickness, i.e., the larger the intercept, the greater the effect of the boundary layer. The values of C and k_D for the linear segments are shown in Table 6. Fig.11. Shows plots of q_t against $t^{1/2}$ for the adsorption processes of MB dye onto DP. In this experiment, the linear line did not pass through the origin, this suggests that the intra-particle diffusion was not the only limiting mechanism in the adsorption process.

Table 6: Intraparticle diffusion parameters for adsorption of MB by DP at 200 ppm

Intraparticle diffusion model			
Adsorbent code	R^2	K_d	Intercept
DP	0.97	0.31501	- 14.08537

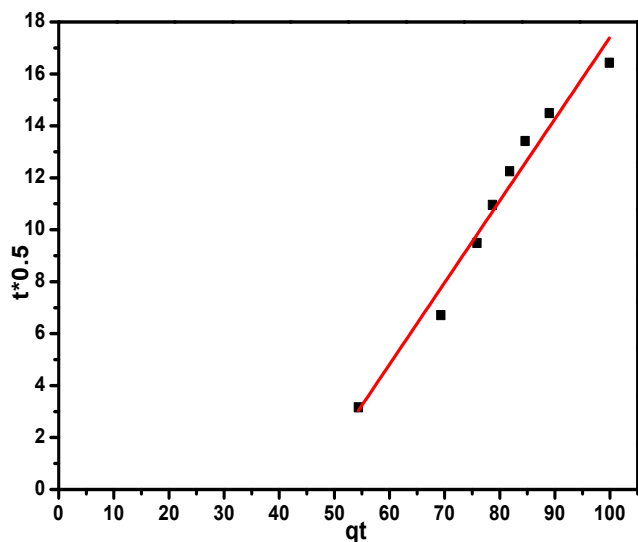


Figure 11: Intra-particle diffusion plots of MB on DP; at 200 ppm for DP.

Evaluation of thermodynamic parameters

The thermodynamic parameters such as change in standard free energy (ΔG°), enthalpy (ΔH°), and entropy (ΔS°) were determined using the following equations [25, 26]:

$$\ln k_d = \frac{\Delta S^\circ}{R} - \frac{\Delta H^\circ}{RT} \quad (9)$$

$$Kd = \frac{q_e}{c_e} \times \rho \quad (10)$$

$$\Delta G^\circ = \Delta H^\circ - T\Delta S^\circ \quad (11)$$

In Eq.(10) the density of the solution ($\rho = 1000 \text{ g/L}$) was used to render Kd dimensionless in order for its logarithmic value to be used for the correct calculation of the thermodynamic parameters. The plot of $\ln kd$ versus $1/T$ was found to be linear as illustrated in Fig.12. The values of ΔS° and ΔH° were calculated from the intercept and slope of linear plot. As seen in Table 7, positive values of ΔH° and negative ΔG° values for all temperatures indicate that MB adsorption on DP is endothermic and spontaneous. The endothermic nature of the adsorption is somehow contradictory to physical adsorption. Generally speaking, it would be expected that the physical adsorption processes

(either from gas or liquid phase) would be exothermic, thus adsorption quantity should decrease with increasing temperature [27, 28]. Barton [29] measuring the enthalpy of adsorption of methylene blue from aqueous solutions onto activated carbon by means of immersion calorimetry found that the actual dye adsorption phenomenon was exothermic. The process however involves the wetting of the sorbent, the endothermic dissociation of the methylene blue dimer, and exothermic exchange reaction between the dye and the adsorbed solvent molecules. Thus the endothermicity of the adsorption process is explained by the necessity of an endothermic dissociation of dye dimers, micelles or aggregates prior to the exothermic adsorption of the dye monomer [30]. In agreement with the results presented in this work MB adsorption has been reported to be endothermic in the literature [31]. Moreover, the positive values of ΔS° point out the increased randomness at the solid/liquid interface during the sorption of dye on DP adsorbent.

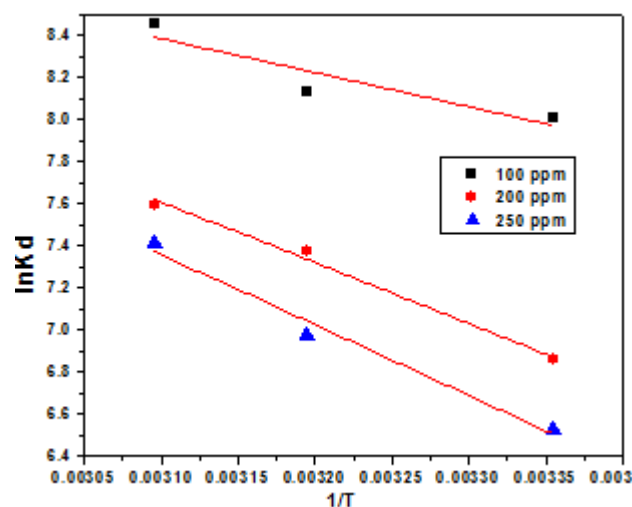


Figure 12: The plots of $\ln K_d$ versus T^{-1} for estimations of thermodynamic parameters of the adsorption process of MB by DP. Condition: ($C_0 = 100\text{--}250 \text{ ppm}$, $T = 25\text{--}50 \text{ }^\circ\text{C}$, adsorbent dose = 0.025 g/25 ml)

Table 7: Thermodynamic parameters for adsorption of MB by DP at different temperatures

Adsorbents	MB Concentration (mg/L)	ΔH° (kJ/mol)	ΔS° (kJ/mol)	ΔG° (kJ/mol)
				298K 313K 323K
DP	600	6.022	0.083	-18.65 -19.89 -20.72

Desorption studies

Desorption of adsorbed MB from spent adsorbent was carried out using different concentration of HCl (0.1-1 M). The adsorbent loaded with 200 ppm of MB at optimum pH was collected and treated with 25 ml XM HCl and agitated till equilibrium to remove the adsorbed MB. It is revealed that for adsorbents DP the percent recovery of MB was about 81.65 % with 0.1 M HCl and the remained constant with the increase of HCl concentration from 0.1 to 1.0 M. L. These results are relatively promising, as the prepared dried papyrus plant could be regenerated for reuse, thus improving their cost-effectiveness and reducing operational cost in water treatment applications.

4. Conclusion

In this study, the adsorption potential of dried papyrus plant for the removal of methylene blue (MB) from aqueous solutions was investigated. The adsorption was studied under varying conditions of initial dye concentration, adsorbent dosage, pH, temperature and the optimum experimental conditions were determined. The DP sample exhibits increased methylene blue adsorption capacity that reached 101.60 mg/g at 298 K , higher than other low cost adsorbents and commercial activated carbons. The MB adsorption capacity increased with the increase of pH in the range of 2–10. The adsorption of MB onto the adsorbents reached equilibrium within about 150 min. The adsorption equilibrium could be well described by Langmuir adsorption isotherms, namely monolayer adsorption on a homogenous

surface. The adsorption kinetics followed a pseudo-second order kinetic model and intra particle diffusion was involved in the adsorption process. Thermodynamic results indicated that the adsorption process was spontaneous and endothermic in nature. MB could be desorbed from dried water hyacinth by using 0.1 M HCl aqueous solution.

References

- [1] F. Banat, N. Al-Bastaki, Treating dye wastewater by an integrated process of adsorption using activated carbon and ultrafiltration, *Desalination*, 170 (2004) 69-75.
- [2] H. Zollinger, *Color chemistry: syntheses, properties, and applications of organic dyes and pigments*, Wiley.com, 2003.
- [3] V. Gupta, A. Mittal, L. Krishnan, V. Gajbe, Adsorption kinetics and column operations for the removal and recovery of malachite green from wastewater using bottom ash, *Separation and Purification Technology*, 40 (2004) 87-96.
- [4] K. Choy, G. McKay, J. Porter, Sorption of acid dyes from effluents using activated carbon, 1999, *Resource, Conservation and Recycling*, 27 57-71.
- [5] K.V. Kumar, Optimum sorption isotherm by linear and non-linear methods for malachite green onto lemon peel, *Dyes and Pigments*, 74 (2007) 595-597.
- [6] Y.-S. Ho, W.-T. Chiu, C.-C. Wang, Regression analysis for the sorption isotherms of basic dyes on sugarcane dust, *Bioresource Technology*, 96 (2005) 1285-1291.
- [7] K. Porkodi, K. Vasanth Kumar, Equilibrium, kinetics and mechanism modeling and simulation of basic and acid dyes sorption onto jute fiber carbon: Eosin yellow, malachite green and crystal violet single component systems, *Journal of hazardous materials*, 143 (2007) 311-327.
- [8] B. Hameed, M. El-Khaiary, Batch removal of malachite green from aqueous solutions by adsorption on oil palm trunk fibre: Equilibrium isotherms and kinetic studies, *Journal of hazardous materials*, 154 (2008) 237-244.
- [9] K.V. Kumar, K. Porkodi, Batch adsorber design for different solution volume/adsorbent mass ratios using the experimental equilibrium data with fixed solution volume/adsorbent mass ratio of malachite green onto orange peel, *Dyes and pigments*, 74 (2007) 590-594.
- [10] C. Namasivayam, R. Radhika, S. Suba, Uptake of dyes by a promising locally available agricultural solid waste: coir pith, *Waste Management*, 21 (2001) 381-387.
- [11] T.-y. Kim, I.-H. Baek, Y.-D. Jeoung, S.-C. Park, Manufacturing activated carbon using various agricultural wastes, *Journal of Industrial and Engineering Chemistry*, 9 (2003) 254-260.
- [12] F. Batzias, D. Sidoras, Dye adsorption by prehydrolysed beech sawdust in batch and fixed-bed systems, *Bioresource Technology*, 98 (2007) 1208-1217.
- [13] R. Malik, D. Ramteke, S. Wate, Adsorption of malachite green on groundnut shell waste based powdered activated carbon, *Waste management*, 27 (2007) 1129-1138.
- [14] M. Šćiban, M. Klačnja, B. Škrbić, Adsorption of copper ions from water by modified agricultural by-products, *Desalination*, 229 (2008) 170-180.
- [15] Owen, Antoinette, and Rachel Danzing. "The history and treatment of the papyrus collection at the Brooklyn Museum." (1993).
- [16] Vaughan, G., *Cyperus papyrus L*, 2011. Available on line on the following link: <http://www.prota4u.org/protav8.asp?p=Cyperus+Papyrus>
- [17] L.J. Kennedy, J.J. Vijaya, G. Sekaran, Effect of two-stage process on the preparation and characterization of porous carbon composite from rice husk by phosphoric acid activation, *Industrial & engineering chemistry research*, 43 (2004) 1832-1838.
- [18] S. Biniak, M. Pakula, G. Szymanski, A. Swiatkowski, Effect of activated carbon surface oxygen-and/or nitrogen-containing groups on adsorption of copper (II) ions from aqueous solution, *Langmuir*, 15 (1999) 6117-6122.
- [19] H. Demiral, İ. Demiral, F. Tımsek, B. Karabacakođlu, Adsorption of chromium (VI) from aqueous solution by activated carbon derived from olive bagasse and applicability of different adsorption models, *Chemical Engineering Journal*, 144 (2008) 188-196.
- [20] N.K. Amin, Removal of reactive dye from aqueous solutions by adsorption onto activated carbons prepared from sugarcane bagasse pith, *Desalination*, 223 (2008) 152-161.
- [21] F.A. Pavan, A.C. Mazzocato, Y. Gushikem, Removal of methylene blue dye from aqueous solutions by adsorption using yellow passion fruit peel as adsorbent, *Bioresource Technology*, 99 (2008) 3162-3165.
- [22] F. HMF, Über die adsorption in lo^o sungen, *Z Phys Chem*, (1906) 385-470.
- [23] E.B. Korngolg, S.; Urtizbera, C., Removal of heavy metals from tap water by a cation exchanger *Desalination* (1996) 104-197.
- [24] E. Fourest, and Roux, J.C., *Applied Microbiology and Biotechnology*, 37 (1992) 399-403.
- [25] M. Tsezos, Remoudaki, E., and Angelatou, V . *International Biodeterioration and Biodegradation* 35 (1997) 129-153.
- [26] W. Weber, J. Morris, Kinetics of adsorption on carbon from solution, *J. Sanit. Eng. Div. Am. Soc. Civ. Eng*, 89 (1963) 31-60.
- [27] D.M. Ruthven, *Principles of adsorption and adsorption processes*, (1984).
- [28] S.S. Barton, The adsorption of methylene blue by active carbon, *Carbon*, 25 (1987) 343-350.
- [29] J.S. Mattson, H.B. Mark, *Activated carbon: surface chemistry and adsorption from solution*, M. Dekker New York, 1971.
- [30] C. Giles, J. Greczek, S. Nakhwa, 19. Studies in adsorption. Part XIII. Anomalous (endothermic) effects of adsorption on inorganic solids, *Journal of the Chemical Society (Resumed)*, (1961) 93-95.
- [31] D. Kavitha, C. Namasivayam, Experimental and kinetic studies on methylene blue adsorption by coir pith carbon, *Bioresource Technology*, 98 (2007) 14-21.